

Polarization of Extrasolar Planets: Sample Simulations

Daphne M. Stam, Joop Hovenier, and Rens Waters

*Astronomical Institute Anton Pannekoek, University of Amsterdam,
Kruislaan 403, 1098 SJ Amsterdam, The Netherlands*

Abstract. Polarization observations appear to be a valuable tool for detecting and studying extrasolar planetary atmospheres. Here, we present numerical simulations of the degree of linear polarization P of starlight reflected by an orbiting planet across the wavelength interval from 0.3 to 3.2 μm , for three types of model atmospheres. The simulations show that P varies with the wavelength and that the variation depends strongly on the atmospheric constituents.

1. Introduction

Although the disk-averaged light emitted by a solar-type star can be considered to be unpolarized, the stellar light that is reflected by a planetary atmosphere will generally be polarized because it has been scattered by gaseous molecules and atmospheric particles. Polarization observations thus appear to be a valuable tool to detect extrasolar planets by separating the light reflected by the planet from the direct starlight.

Polarization observations could also be used to derive information about extrasolar planetary atmospheres. Namely, as is known from observations of solar system planets (see e.g., Hansen & Hovenier (1974)) and from numerical simulations for extrasolar planets (Seager et al. 2000), the degree of (linear) polarization P of light reflected by a planet will depend on various parameters, such as the phase angle (the angle between star, planet, and observer), and the planet's atmospheric structure and composition. Through the optical properties of the atmospheric constituents, P also depends on the wavelength λ of the light. Indeed, the spectral distribution of P consists generally of a smoothly varying continuum with superimposed high-spectral resolution features due to gaseous absorption bands and Raman scattering (Aben et al. 2001).

In this paper, we present and discuss the simulated continuum wavelength dependence of P between 0.3 and 3.2 μm for three different extrasolar planetary model atmospheres.

2. Radiative Transfer Calculations

The degree of linear polarization of starlight reflected by a planet is defined as $P = (I_r - I_l)/(I_r + I_l)$, with I_l and I_r the radiances (intensities) of light polarized parallel and perpendicularly to the plane containing the observer, and the centers of the star and the planet. I_l , I_r , and P generally depend on the

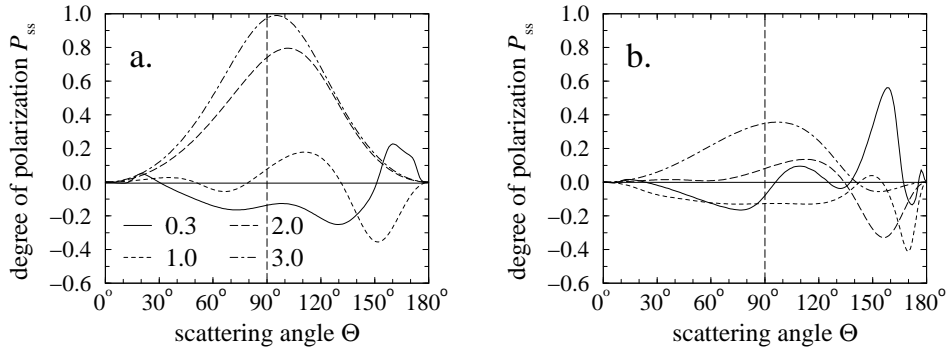


Figure 1. The degree of polarization of light singly scattered by (a) the small and (b) the large cloud particles, for $\lambda = 0.3, 1.0, 2.0,$ and $3.0 \mu\text{m}$.

illumination and viewing geometries of the planetary atmosphere, and on the vertical distribution and optical properties of the atmospheric constituents.

We use an adding–doubling algorithm (de Haan et al. 1987) to calculate P between 0.3 and $3.2 \mu\text{m}$. Locally, the planetary atmosphere is modeled as a stack of 38 plane–parallel, homogeneous layers, bounded below by a non–polarizing and isotropically reflecting layer with albedo A . The pressure varies from 5.6 bars at the bottom to 0.0001 bars at the top of the atmosphere. By way of example, we use Neptune’s temperature profile (Lindal 1992). For each atmospheric layer and wavelength, the molecular scattering optical thickness, τ_m , is calculated from the atmospheric pressure and temperature profile (Stam et al. 1999). Molecular absorption is ignored. Our ‘clear’ model atmosphere contains only molecules.

Besides molecules, an atmospheric layer can contain cloud particles. We consider two ‘cloudy’ atmospheres, in which the layers up to 0.75 bars (where the temperature is 65.4 K) contain either small or large cloud particles. At $2.0 \mu\text{m}$, the cloud optical thickness of both model atmospheres is 43. The cloud optical thickness of an atmospheric layer is calculated from the user defined particle number density and the wavelength dependent particles’ extinction cross–section. This cross–section and the particles’ scattering matrix are calculated using Mie–theory, assuming a wavelength independent refractive index of 1.4. In the visible, this is representative for condensates thought to be present in an atmosphere like Neptune’s. The particles’ single scattering albedo thus equals 1. Both the small and the large cloud particles are distributed in size according to a gamma distribution (Hansen & Travis 1974), with an effective variance of 0.1 and effective radii of $0.5 \mu\text{m}$ and $1.0 \mu\text{m}$, respectively. Figure 1 shows the degree of polarization P_{ss} of light that has been singly scattered by the cloud particles for four different wavelengths. Note that at $\lambda = 3.0 \mu\text{m}$, P_{ss} of the small particles is similar to (the wavelength independent) P_{ss} of molecules.

For the three model atmospheres described above, we calculate I_1 and I_r , and from these P , for three locations on the light equator of a planet at a phase angle of 90° . For each of these locations, Table 1 lists the longitude (measured from the sub–observer longitude), the local stellar zenith angle θ_0 , the local

Table 1. Longitude, θ_0 , θ , and Θ for three locations on the planet.

Nr.	Long.	θ_0	θ	Θ
1	30°	60°	30°	90°
2	45°	45°	45°	90°
3	60°	30°	60°	90°

viewing angle θ (measured between the local vertical and the direction of the reflected light), and the local single scattering angle Θ .

3. Results

Figure 2 shows P as a function of λ for the three locations on the planet. For the clear model atmosphere (Figure 2a), we show results for $A = 0.0$ and 0.05 . The cloudy atmospheres (Figure 2b) are bounded below by black layers ($A = 0.0$). According to Figure 2, P is little sensitive to θ or θ_0 for the model atmospheres studied here. Indeed, P is mostly determined by the single scattering angle Θ , which is 90° for all three locations (this suggests that these local values of P are representative for the planetary disk).

The wavelength dependence of P clearly depends on the model atmosphere and albedo A . When the clear atmosphere (Figure 2a) is bounded below by a black layer, P increases smoothly from about 0.25 at $\lambda = 0.3 \mu\text{m}$ to 0.95 at $3.2 \mu\text{m}$. When $A = 0.05$, P reaches a maximum of about 0.6 at $\lambda = 1.3 \mu\text{m}$ and decreases to about 0.07 at $\lambda = 3.2 \mu\text{m}$. For the two cloudy atmospheres (Figure 2b), P is about 0.25 at $\lambda = 0.3 \mu\text{m}$ (like for the clear atmosphere), decreases to about 0.05 at $\lambda = 1.2 \mu\text{m}$ for the atmosphere with small cloud particles, and to about 0.02 at $1.5 \mu\text{m}$ when the particles are large. Towards longer wavelengths, P increases up to about 0.3 and 0.1 for the small and large particles, respectively.

The spectral behaviour of P can be explained by considering the wavelength dependence of the atmospheric optical thickness, the single scattering degree of polarization P_{ss} , and the albedo A . At $\lambda = 0.3 \mu\text{m}$, the atmospheric molecular scattering optical thickness, τ_{m} , is large, namely 160 (of which 20 above the cloud layers). As a result, most of the reflected light is multiple scattered light from the top layers of the atmosphere. Because all three model atmospheres have only molecules in their top layers, they yield similar values of P , namely 0.25. This value is much lower than P_{ss} of the molecules at $\Theta = 90^\circ$, because multiple scattering dilutes P .

With increasing wavelength, τ_{m} and with it the multiple scattering in the molecular atmospheric layers, decreases rapidly ($\tau_{\text{m}} \propto \lambda^{-4}$). As a result, P pertaining to the clear atmosphere (Figure 2a) with $A = 0.0$, increases towards $P_{\text{ss}} \approx 1.0$ at the longest wavelengths. The decrease of P with wavelength in case $A = 0.05$, is due to the increasing contribution of unpolarized light from below the atmosphere to the reflected light at the top of the atmosphere. In the cloudy atmospheres (Figure 2b), the decrease of τ_{m} increases the contribution of

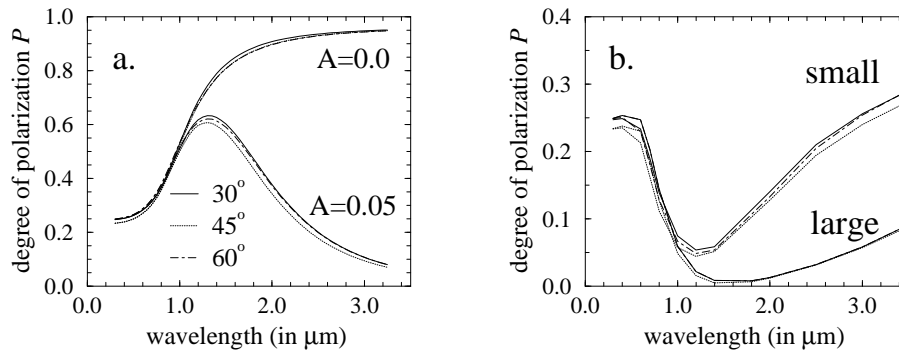


Figure 2. Degree of polarization of light reflected by (a) the clear and (b) the cloudy model atmospheres as a function of wavelength for the three locations on the planet indicated by their longitudes. The slightly uneven appearance of the curves in (b) is due to the limited spectral resolution of these simulations.

light scattered in the lower atmospheric layers that contain the cloud particles, especially because the optical thickness of the cloud layers decreases less rapidly with λ than that of the molecular layers. The low values of P that occur around $\lambda = 1.2 \mu\text{m}$ and $1.5 \mu\text{m}$ for respectively the small and the large cloud particles, are thus largely due to light that has been scattered by the cloud particles, not only because this light is multiple scattered light, but also because at these wavelengths, P_{ss} of the cloud particles is small (see Figure 1). With increasing λ , multiple scattering decreases, and P is increasingly determined by (the wavelength dependent) P_{ss} of the cloud particles. For the atmosphere containing the small cloud particles, P increases more than for the atmosphere with the large particles, mostly because P_{ss} of the small particles increases more with λ than that of the large particles (see Figure 1).

4. Conclusions

Our numerical simulations show that P of light reflected by extrasolar planets can vary strongly with wavelength and atmospheric composition. More knowledge on this wavelength dependence is crucial both for the development of polarimeters designed to detect extrasolar planets and for the analysis of polarimetric observations.

References

- Hansen, J. E. & Hovenier, J. W. 1974, *J. Atmos. Sci.*, 31, 1137
Hansen, J. E. & Travis, L. D. 1974, *Space Sci. Rev.*, 16, 527
Seager, S., Whitney, B. A., & Sasselov, D. D. 2001, *ApJ*, 540, 504
Aben, I., Stam, D. M., & Helderma, F. 2001, *Geophys. Res. Lett.*, 28, 519
De Haan, J. F., Bosma, P. B., & Hovenier, J. W. 1987, *A&A*, 183, 371
Stam, D. M., De Haan, J. F., Hovenier, J. W. & Stammes, P. 1999, *J. Geophys. Res.*, 104, 16843
Lindal, G. F. 1992, *AJ*, 103, 967